ABSENCE OF CONJUGATION IN VIBRATIONAL SPECTRA AND ASSIGNMENTS OF DICHLORO(VINYL)PHOSPHINE AND DICHLORO(PHENYL)PHOSPHINE OXIDES AND SULFIDES

Wolfgang FÖRNER* and Hassan M. BADAWI

Department of Chemistry, King Fahd University of Petroleum & Minerals (KFUPM), Dhahran 31261, Saudi Arabia; e-mail: forner@kfupm.edu.sa

Dedicated to Professor Rudolf Zahradnik on the occasion of his 80th birthday.

The structure and conformational stability of dichloro(vinyl)phosphine and dichloro(phenyl)-phosphine oxides and sulfides were investigated using calculations at the DFT/6-311G** and ab initio ones at the MP2/6-311G** level. We know from our previous results that the addition of diffuse functions to a valence triple zeta basis with polarization functions might lead to an unbalanced basis, which performs even worse than the smaller basis without diffuse functions, as it is the case for the 6-311++G** basis set in the Gaussian program. For large energy differences between conformers, DFT works very well, in some cases even better than MP3 or MP4. The vinyl derivatives were predicted to exist in a cis/gauche conformational equilibrium with cis (the PX bond, X being oxygen or sulfur eclipses the vinyl groups) being the predominant conformer at ambient temperature. In the phenyl case case the two planar forms are equivalent minima. The asymmetric potential function for the internal rotation was determined for each of the molecules. The vibrational frequencies were computed and the spectra, where possible, were compared with the experimental ones. Normal coordinate calculations were carried out and potential energy distributions were calculated for the molecules in the cis and gauche conformations (in the vinyl case, planar one for phenyl), providing a complete assignment of the vibrational lines to symmetry coordinates in the molecules. From our results and their analysis we conclude, in agreement with literature results based on localized orbitals, that conjugation effects are absent – or at least negligible – as compared with electrostatic ones in determining the structures of the stable conformers in both the vinyl and the phenyl derivatives. The P–O bond should be a highly polarized triple bond, as confirmed by analysis of Mulliken populations. The polarization turned out to be much less in the sufides due to the much smaller electronegativity of sulfur as compared with oxygen.

Keywords: DFT and MP2 calculations; Normal coordinate analyses; Vibrational assignments and spectra; Torsional potentials; Dichloro(vinyl)phosphine oxide and sulfide; Dichloro-(phenyl)phosphine oxide and sulfide.

Over the past years, the conformational behavior and structure of many conjugated vinyl compounds with the general formula of $R_2C=CRCXO$, where $X = F$ or Cl and $R = H$ or CH_3 was reported[1–12]. Conjugation effects in these molecules generally tend to stabilize the planar cis and trans conformers but not the non-planar gauche conformations and lead to a high rotational barrier as compared with the saturated analogs. In propenoyl halides both the halogen and oxygen atoms of the carbonyl group play a competitive role in determining the conformational equilibrium, which leads to a small energy difference between the stable conformers of the molecules. In the case of 2-fluoropropenoyl fluoride[7,11] and 2-chloro-propenoyl fluoride[8], the trans conformer with the two halogen atoms directed away from each other was determined to be more favorable than the cis conformer. Furthermore, the presence of the methyl group was shown to significantly influence the direction of the conformational equilibrium in the methyl-substituted propenoyl halides. For 2-methyl-2-butenoyl fluoride and chloride, the trans forms were found to be the lower energy conformer, while for 3-methyl-2-butenoyl fluoride and chloride, the cis conformers were determined to be the low-energy conformers[12,13].

Some years ago we reported the study of conformational and structural stability of ethenesulfonyl chloride $CH_2=CHSO_2Cl$ and fluoride $CH_2=CHSO_2F$ [14] for their great chemical importance and structural interest[15]. The molecules were predicted to exist predominantly in the non-planar gauche conformations with the vinyl C=C group nearly eclipsing one of the sulfonyl S=O groups, again as a result of significant conjugation between the two groups[14].

As a continuation of our interest in conjugated molecular systems we investigate in the present work the conformational behavior and structural stability of dichloro(vinyl)phosphine oxide, $CH_2=CHPCl_2O$ and sulfide, $CH_2=CHPCl_2S$, as well as the corresponding compounds with phenyl substituent, dichloro(phenyl)phosphine oxide, $C_6H_5–PCl_2O$, and sulfide, $C_6H_5–PCl_2S$. We carried out DFT and ab initio MP2 optimizations[16] of the energies for the stable conformers of the molecules. From the data the relative conformational stabilities were determined. We can conclude that conjugation effects are almost absent in all of the compounds, and that their stabilities are mainly determined by electrostatic and possibly, probably not, steric effects. Additionally, vibrational frequencies were calculated on the DFT level. Complete assignment was made for all the normal modes by employing normal coordinate calculations following[17]. Experience tells us that in cases of larger energy differences between conformers (kcal/mol), DFT works rather well, in some cases even better than MP3 or MP4. Furthermore, DFT can predict vibrational spectra very well as compared with ex-

periments, even in cases where energy differences are not so large. We also used the vibrational data to make plots for the vibrational IR and Raman spectra of the molecules. The results of this work are presented here and, where possible, compared with experimental spectra. Thus, for three of our systems we can make comparisons with experiment and give reliable assignments of the observed modes, while for dichloro(phenyl)phosphine sulfide, we present a theoretical prediction of the vibrational spectra and the assignment of the spectral lines, which is also reliable. Also comparisons with the spectra of propenoyl halides[18] and (fluoromethyl)phosphonic dichloride[19] are in principle possible. However, having the spectra of the compounds, we decided to resort to them. The Raman intensities were calculated as given in the literature[20,21]. Our interest in organophosphorus compounds actually arose because of the tremendous importance of such compounds in chemistry[19,22–25]. Importantly, such phosphorus compounds have become very interesting for the chemical industry as, e.g., starting materials for drug synthesis, as polymer additives, flame retardants, and metal extractants[26].

For our calculations we used the valence triple zeta basis set with polarization functions on all atoms, i.e. 6-311G**. Our previous calculations[27,28] have suggested that this basis set is superior to the larger 6-311+G** or 6-311++G** basis sets which include diffuse functions and do not seem to be well balanced, indicated by warnings about large MO coefficients in the Gaussian outputs, suggesting the presence of linear dependencies in the basis set, which would make the actual calculations not very meaningful. This holds just for the 6-311+G** and 6-311++G** basis sets in the Gaussian program system but is not true in general for any basis set that includes diffuse functions. However, the smaller 6-311G** basis works quite well in a series of halo and dihalo(vinyl) methanes, silanes, and germanes.

DFT AND ab initio CALCULATIONS

The Gaussian 98 program[16] running on an IBM RS/6000 43P model 260 workstation, was used to carry out the LCAO-MO-SCF calculations at the DFT and MP2/6-311G** levels. The structures of the molecules in their most stable conformations together with the atom numbering are shown in Fig. 1.

They were optimized by minimizing the energy with respect to all the geometrical parameters. The calculated structural parameters, total energies, rotational constants and dipole moments of the molecules are listed in Tables 1S and 2S (S for Supplementary material). The calculations of the vinyl derivatives (VO and VS) showed the existence of a cis (c) to gauche (g)

conformational equilibrium with the cis form being the predominant conformer at ambient temperature. Experimental geometrical data were taken from[29]. The energy differences between the two conformers were calculated to range between 1.5 and 2 kcal/mol, with a cis-gauche rotational barrier – through a gauche transition state – of ca. 3 kcal/mol for the vinyl compounds. The phenyl derivatives (PO and PS) show two, structurally equivalent, stable planar (p) conformers with the same energies, the rotational barriers over the perpendicular (pp) transition states (TS) being around 2–3 kcal/mol. We have also performed MP3, MP4-SDQ, CCSD, and CCSD(T) calculations. However, we are not able to perform geometry optimizations on these levels of theory with our computers, and thus we had to perform these calculations only on the vinyl derivatives and using the geometry optimized by MP2. The results are given in Table I.

As obvious from the table ab initio energy differences and barrier heights are comparable to each other and mostly somewhat larger than DFT results. However, the changes in going from DFT to CCSD(T) amount to ca. 0.3 kcal/mol at most. Thus we conclude that our results of higher level test calculations do not affect at all our conclusions reached below based on DFT energies.
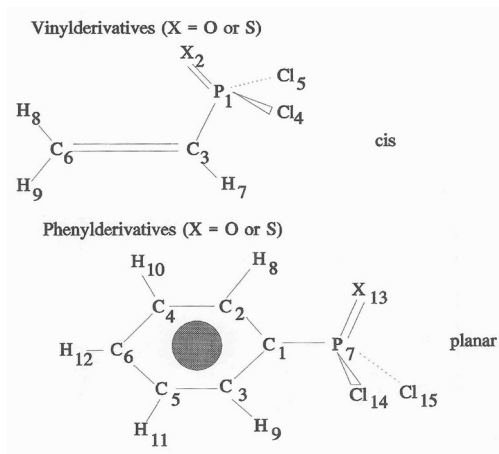

FIG. 1
Atom numbering in the vinyl- and phenylphosphine derivatives under study

Total energies of the cis (c) and gauche (g) conformers and the transition state (TS) (in hartree) for dichloro(vinyl)phosphine oxide and sulfide, together with the relative energies of gauche (relative to cis), ΔE (in kcal/mol), and the barriers to cis→gauche rotation, E_b (in kcal/mol), calculated with the 6-311G** basis set using DFT, MP2 (both including geometry optimization), MP3, MP4(SDQ), CCSD, and CCSD(T) (the latter four were calculated at the MP2 optimized geometries)

Method	c	TS	g	ΔE	ΔE_b
		Dichloro(vinyl)phosphine oxide			
DFT	−1415.1480160	−1415.1427759	−1415.1448080	2.01	3.29
MP2	−1413.0395096	−1413.0343248	−1413.0358988	2.27	3.25
MP3	−1413.0692994	−1413.0636745	−1413.0653334	2.49	3.53
MP4(SDQ)	−1413.0839272	−1413.0786570	−1413.0817670	2.35	3.31
CCSD	−1413.0815537	−1413.0761076	−1413.0776328	2.46	3.42
CCSD(T)	−1413.1159161	−1413.1107538	−1413.1122076	2.33	3.24
		Dichloro(vinyl)phosphine sulfide			
DFT	−1738.1095468	−1738.1053598	−1738.1073109	1.40	2.63
MP2	−1735.6094466	−1735.6051787	−1735.6066504	1.75	2.68
MP3	−1735.6554788	−1735.6513365	−1735.6527201	1.73	2.60
MP4(SDQ)	−1735.6647426	−1735.6606630	−1735.6620147	1.71	2.56
CCSD	−1735.6637431	−1735.6596583	−1735.6609623	1.74	2.56
CCSD(T)	−1735.6976877	−1735.6937740	−1735.6950289	1.67	2.46

Torsional Potential Function

The potential function scan for the internal rotation about the C–C single bond was obtained by allowing the CCPO dihedral angle (Φ) to vary by 15° increments from 0° (cis position) to 180° (trans position). Full geometry optimization at each of the fixed CCPO dihedral angles (φ) of 15, 30, 45, 75, 90, 105, 135, 150, and 165° were carried out at the DFT and MP2/6-311G** level of calculations. The barriers to internal rotation in the molecules were calculated and listed also in Tables 1S and 2S (see also Table III for more de-

tails). The torsional potential function was represented as a Fourier cosine series of the dihedral angle (Φ):

$$v(\phi) = V_0 + \sum_{n=1}^{N} \frac{V_n}{2} \left[1 - \cos(n\phi) \right] \qquad (1)$$

where the potential coefficients from V_0 to V_6 ($N = 6$) are considered adequate to describe the potential function (as shown by the root-mean-square deviations, rms, of the least-square fitting). The results of the energy optimizations were used to calculate the six coefficients by least-squares fitting (Table II, while coefficients obtained using a 6-311++G** basis set are given in Table 3S). To get the real total energies in hartree, one has to include the total energy to which all the fit functions are relative (see the corresponding figure legends).

Fig. 2
MP2 potential scans along the $X_2P_1C_3C_6$ (X = O or S) dihedral angle for dichloro(vinyl)phosphine oxide (the actually calculated points are hexagons for 6-311G** and diamonds for 6-311+G** basis set) and sulfide (the actually calculated points are triangles for 6-311G** and asterisks for 6-311+G** basis set). In 6-311G** basis set, the oxide curve is relative to –1413.039510 hartree while the sulfide curve is relative to –1735.609447 hartree in 6-311+G** basis set, the oxide curve is relative to –1413.056652 hartree while the sulfide curve is relative to –1735.626517 hartree

The potential functions for the internal rotation in the vinyl derivatives (Figs 2 and 3) were consistent with those with two minima at cis ($\Phi = 0°$) and gauche ($\Phi = 130°$) positions. However, the calculations show that the

TABLE II
Potential constants V_n (in kcal/mol) obtained in the various fits of the rotational potentials for dichloro(vinyl)phosphine oxide (VO) and sulfide (VS), and for dichloro(phenyl)phosphine oxide (PO) and sulfide (PS) as calculated using DFT/B3LYP and MP2 methods with the 6-311G** basis and the root-mean-square deviations, rms (in cal/mol), of the fits are given (see Eq. (1))

n	VO		VS	
	V_n(DFT)	V_n(MP2)	V_n(DFT)	V_n(MP2)
0	−0.0032	0.0003	0.0081	0.0024
1	1.2486	1.5791	0.9040	1.3299
2	1.4807	1.3787	1.0146	0.9580
3	1.6813	1.5869	1.5410	1.4589
4	0.0044	0.0898	−0.0230	0.0696
5	0.0228	−0.0084	−0.0032	−0.0189
6	−0.0133	−0.0127	−0.0131	0.0039
rms, cal/mol	3.13	1.26	8.91	2.08

n	PO		PS	
	V_n(DFT)	V_n(MP2)	V_n(DFT)	V_n(MP2)
0	0.0045	−0.0011	0.0033	0.0089
1	0.0	0.0	0.0	0.0
2	2.8418	2.6064	1.7420	1.7432
3	0.0	0.0	0.0	0.0
4	0.1450	0.2159	0.2119	0.3092
5	0.0	0.0	0.0	0.0
6	0.0076	−0.0370	0.0281	0.0176
rms, cal/mol	7.33	4.07	4.90	7.19

cis conformer is quite lower in energy than the gauche form as shown in Figs 2 and 3. As Table 3S indicates the use of a 6-311++G** basis set in MP2 calculations, results in no pronounced changes.
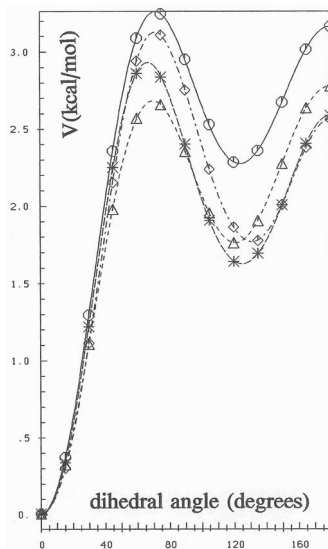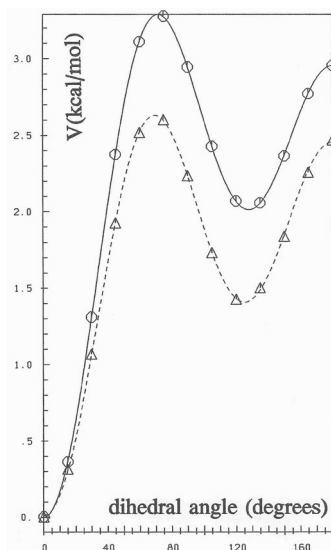

FIG. 3

Potential scans along the $X_2P_1C_3C_6$ (X = O or S) dihedral angle for dichloro(vinyl)phosphine oxide (the actually calculated points are hexagons) and sulfide (the actually calculated points are triangles) calculated by the DFT/B3LYP method and with the 6-311G** basis set. The oxide curve is relative to –1415.148021 hartree while the sulfide curve is relative to –1738.109552 hartree

For the phenyl derivatives, the potentials are symmetric with respect to the perpendicular TS (90°) as shown in Fig. 4. In Fig. 4 we show the corresponding potential function for the phenyl derivatives which are symmetric around a dihedral angle of 90°.

Again, there are no pronounced differences between the MP2 and the DFT calculations. The potential constants are given again in Table II. However, as expected, the barriers for the sulfide are much lower than those for the oxide, because a S atom, being less electronegative than an O atom, leads to a much smaller charge separation in the P–S bond as compared with the P–O bond (see below for further details).

In Table III we list the cis-gauche and gauche-cis rotational barriers for the vinyl and the planar-to-planar (via the perpendicular transition state) barriers for the phenyl derivatives.

For comparison, we calculated the trans-cis and cis-trans barriers for butadiene using the same method and basis set because butadiene is a molecule where conjugation exists, while in our compounds the importance of conjugation effects is doubtful[30]. Obviously, the rotational barriers are much smaller in VO and VS than they are in butadiene, suggesting that conjugation is much less important in these compounds than it is in butadiene, where the rotation involves the breaking of a partial C=C π-bond. In the phenyl derivatives, the barriers are much smaller, since conjugation there would involve a reduction of the aromatic character of the benzene rings. The fact that in both cases the barriers are much smaller for the sulfides than for the oxides suggests that the major effects determining the structure should be electrostatic since the P–S bond is much less polarized than the P–O bond (see Table 4S which gives the Mulliken populations). If steric effects were to be more dominant, again the larger sulfur atom should have a larger effect.
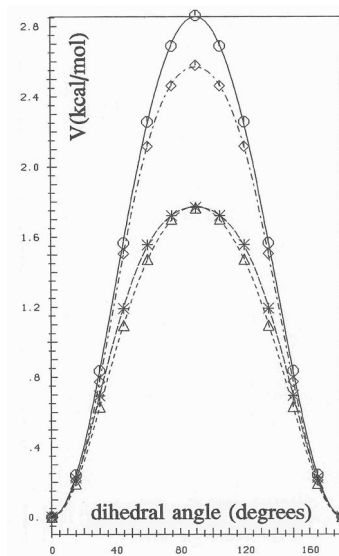
FIG. 4

DFT and MP2 potential scans (both in 6-311G** basis set) along the $X_{13}P_7C_1C_3$ (X = O or S) dihedral angle for dichloro(phenyl)phosphine oxide (the actually calculated DFT points are hexagons while diamonds are for MP2) and sulfide (the actually calculated DFT points are triangles while asterisks are for MP2). For DFT, the oxide curve is relative to –1568.840000 hartree while the sulfide curve is relative to –1891.800715 hartree. For MP2, the oxide curve is relative to –1566.275405 hartree while the sulfide curve is relative to –1888.846193 hartree

TABLE III
Rotational barriers (in kcal/mol) as computed by the DFT/B3LYP method using the 6-311G** basis set for butadiene, dichloro(vinyl)phosphine oxide (VO) and sulfide (VS), and dichloro(phenyl)phosphine oxide (PO) and sulfide (PS), where p denotes the stable planar conformer, pp the perpendicular one (transition state)

Compound	trans→cis	cis→trans
Butadiene	7.17	3.14
	cis→gauche	gauche→cis
VO	3.29	0.94
VS	2.63	1.06
	p→p (via pp)	
PO	2.86	
PS	1.76	

To have a clearer insight into possible conjugation effects, we list the bond lengths in butadiene, VO, VS, PO, and PS (Table IV).

The numbers between a stable conformer and the transition state show the increase in bond length in % when going from the conformer to the TS. In butadiene, the two conjugated C=C double bonds are little shortened in the TS, however, the central C–C bond length increases by 2.1% between the trans conformer and the TS and by 1.1% between the cis conformer and the TS. On the other hand, in VO, VS, PO or PS, the C–P bond length increases by at most 0.7% when going from the cis conformer to the TS (VO, VS) or from planar conformers to the TS (PO, PS). Thus, also the look at the bond length changes as compared with butadiene confirms again that in VO, VS, PO, and PS, conjugation effects are negligible, if present at all. Indeed, in[30], in a study of localized orbitals the authors arrived at the conclusion that the P–O bond actually is not a double bond, but rather a triple bond with large negative (O) and positive (P) partial charges. These partial charges are considerably reduced in the case of P–S bonds (Table 4S).

A quantity that should be directly proportional to the rotation potentials, if their origins were of exclusively electrostatic origin, would be X:

TABLE IV
Bond lengths (in Å) as optimized by the DFT/B3LYP method using a 6-311G** basis set in the stable conformers (cis, gauche or planar (p)) and transition states (TS or perpendicular (pp)) for rotation in butadiene, dichloro(vinyl)phosphine oxide (VO) and sulfide (VS), and dichloro(phenyl)phosphine oxide (PO) and sulfide (PS). Bonds are $C_6=C_3$, C_3-P_1 and $P_1=X_2$ in VO (X = O) and VS (X = S), and $C_2=C_1$ (in the ring), C_1-P_7 and $P_7=X_{13}$ in PO (X = O) and PS (X = S). The percentages between bond lengths give the change of them when going from the stable conformer to the TS

Parameter	C=C	C–C	C=C
s-trans	1.336	1.456	1.336
	–0.4%	+2.1%	–0.4%
TS	1.330	1.486	1.330
	–0.4%	+1.1%	–0.4%
s-cis	1.336	1.470	1.336
	C=C	C–P	P=X
s-cis-VO	1.330	1.794	1.471
	–0.08%	+0.7%	0.0%
TS	1.329	1.806	1.471
	0.0%	+0.4%	0.0%
s-gauche-VO	1.329	1.798	1.471
s-cis-VS	1.329	1.805	2.920
	–0.05%	+0.5%	0.0%
TS	1.328	1.814	1.920
	0.0%	+0.5%	0.0%
s-gauche-VS	1.328	1.805	1.920
	C=C (ring)	C–P	P=X
p-PO	1.396	1.803	1.472
	+0.07%	+0.7%	0.0%
pp-PO (TS)	1.397	1.815	1.472
p-PS	1.396	1.818	1.922
	+0.07%	+0.06%	–0.2%
pp-PS (TS)	1.397	1.819	1.919

TABLE V
The quantities X and their values relative to the corresponding smallest one, $100 \times X_r$ (both in Å^{-1}), and the total energies E_t (in kcal/mol) relative to the most stable conformer for dichloro(vinyl)phosphine oxide and sulfide, and for dichloro(phenyl)phosphine oxide and sulfide. TS denotes transition state, p the planar and pp the perpendicular conformers, respectively

Quantity	cis	TS	gauche
	Dichloro(vinyl)phosphine oxide		
X	−0.5821	−0.5440	−0.5479
$100 \times X_r$	0.00	3.81	3.42
E_t	0.00	3.29	2.01
	Dichloro(vinyl)phosphine sulfide		
X	−0.2561	−0.2306	−0.2340
$100 \times X_r$	0.00	2.55	2.21
E_t	0.00	2.63	1.40

Quantity	p	pp
	Dichloro(phenyl)phosphine oxide	
X	−0.5928	−0.5273
$100 \times X_r$	0.00	6.55
E_t	0.00	2.86
	Dichloro(phenyl)phosphine sulfide	
X	−0.2567	−0.2063
$100 \times X_r$	0.00	5.04
E_t	0.00	1.76

$$X = \sum_{i=2}^{N} \sum_{j=1}^{i-1} \frac{Q_i Q_j}{R_{ij}} = \frac{4\pi\varepsilon_0}{e^2} E_{st} \qquad (2)$$

and X_r would be its value relative to the smallest one (cis for VO and VS, and p for PO and PS). In Eq. (*2*), ε_0 is the permittivity of the vacuum, e the absolute value of the electronic charge, Q_i the Mulliken charge on atom i (multiples of e), R_{ij} the distance between atoms i and j, and N the number of atoms in the molecule. E_{st} is the electrostatic interaction energy between these charges in a molecule. In Table V the values are shown together with the total energies relative to the most stable conformer, E_t, for the sequence cis-TS-gauche for VO and VS and p-pp for PO and PS.

Obviously the sequence of X_r numbers parallels that of E_t. The differences in the numbers are definitely due to the different units and might also be due in part to the well-known shortcomings of Mulliken's population analysis. However, Table V points strongly to the direction of the mostly electrostatic origin of stabilities of the conformers. Any major influence of conjugation effects appears highly unlikely according to the arguments given above. Also conjugation effects would stabilize the trans form, instead of gauche, but trans is a transition state in the vinyl compounds.

Vibrational Frequencies and Normal Coordinate Analyses

Our molecules in their most stable conformations have C_s symmetry. The vibrational modes span the irreducible representations 14 A'+ 7 A″ in the vinyl case and 26 A′ + 13 A″ in the phenyl case. The A′ modes should be polarized, while the A″ modes depolarized in the Raman spectra of the liquid. The vinyl molecules in the gauche conformations have C_1 symmetry and the vibrational modes span the irreducible representation 21 A and should be polarized in the Raman spectra of the liquids.

Normal coordinate analyses were carried out for the stable cis, gauche or planar conformers of the molecules in order to provide a complete assignment of the fundamental vibrational frequencies. Note, that the theoretical frequencies have been computed in the harmonic approximation by the Gaussian program. A computer program was written for this purpose following Wilson's method[17]. The Cartesian coordinates for the stable conformers together with the normal modes (in Cartesian coordinates) and the frequencies from the Gaussian 98 output were used as input in the program. An over-complete set of internal coordinates (Table 5S for vinyl and Table 6S for phenyl derivatives) was used to form symmetry coordinates

(Table VI for vinyl and Table VII for phenyl derivatives). Our program auto-matically detects redundant internal coordinates and eliminates them from the symmetry coordinates.

Following that, the potential energy distribution (PED) for each normal mode among the symmetry coordinates of the molecules in their stable conformations was calculated. A complete assignment of the fundamentals was proposed. The assignments were made based on calculated PED, infra-red band intensities, Raman line activities, and depolarization ratios. The

TABLE VI
Symmetry coordinates for dichloro(vinyl)phosphine oxide (X = O) and sulfide (X = S), where symmetries are for the cis conformation (not normalized)

Species		Description	Symmetry coordinate
A′	C–H	stretch	$S_1 = S$
	CH_2	antisymmetric stretch	$S_2 = P_1 - P_2$
	CH_2	symmetric stretch	$S_3 = P_1 + P_2$
	PCl_2	symmetric stretch	$S_4 = X_1 + X_2$
	C–P	stretch	$S_5 = Q$
	P=X	stretch	$S_6 = T$
	C=C	stretch	$S_7 = R$
	CH_2	deformation (scissor)	$S_8 = 2\alpha_1 - \alpha_2 - \alpha_3$
	CH_2	wag	$S_9 = \alpha_2 - \alpha_3$
	PCl_2	rock	$S_{10} = \varepsilon_1 - \varepsilon_2 + \pi_1 - \pi_2$
	PCl_2	deformation (scissor)	$S_{11} = 4\delta - \varepsilon_1 - \varepsilon_2 - \pi_1 - \pi_2$
	CPX	bend	$S_{12} = 5\theta - \varepsilon_1 - \varepsilon_2 - \pi_1 - \pi_2 - \delta$
	CCP	bend	$S_{13} = 2\beta_1 - \beta_2 - \beta_3$
	CH	bend (in-plane)	$S_{14} = \beta_2 - \beta_3$
A″	PCl_2	antisymmetric stretch	$S_{15} = X_1 - X_2$
	PCl_2	wag	$S_{16} = \varepsilon_1 + \varepsilon_2 + \pi_1 - \pi_2$
	PCl_2	twist	$S_{17} = \varepsilon_1 - \varepsilon_2 + \pi_1 + \pi_2$
	CH	bend (out-of-plane)	$S_{18} = \omega$
	CH_2	deformation I	$S_{19} = \xi_1$
	CH_2	deformation II	$S_{20} = \xi_2$
		antisymmetric torsion	$S_{21} = \tau$

data of the vibrational assignments are given in Tables VIII–X. The experimental spectra for VO [31] and VS [32] are given in the references in tabular form; so in Tables VIII and IX the experimental wavenumbers are also given together with the error percentages of the ones calculated by DFT.

TABLE VII
Symmetry coordinates (not normalized; $\Phi = +15°$) for dichloro(phenyl)phosphine oxide (X = O) and sulfide (X = S)

Species		Description	Symmetry coordinate
A′	β-CH	antisymmetric stretch	$S_1 = r_3 - r_{11}$
	β-CH	symmetric stretch	$S_2 = r_3 + r_{11}$
	γ-CH	antisymmetric stretch	$S_3 = r_5 - r_9$
	γ-CH	symmetric stretch	$S_4 = r_5 + r_9$
	δ-CH	stretch	$S_5 = r_7$
	ring-P	stretch	$S_6 = A$
	β-CH	bend (in-plane)	$S_7 = \nu_1 - \nu_2 + \nu_3 - \nu_4$
	β-CH	bend (in-plane)	$S_8 = \nu_1 - \nu_2 - \nu_3 + \nu_4$
	γ-CH	bend (in-plane)	$S_9 = \nu_5 - \nu_6 + \nu_7 - \nu_8$
	γ-CH	bend (in-plane)	$S_{10} = \nu_5 - \nu_6 - \nu_7 + \nu_8$
	δ-CH	bend (in-plane)	$S_{11} = \nu_9 - \nu_{10}$
	ring	breathing	$S_{12} = R_1 + R_2 + R_3 + R_4 + R_5 + R_6$
	ring	deformation	$S_{13} = R_1 + R_2 - 2R_3 + R_4 + R_5 - 2R_6$
	ring	deformation	$S_{14} = R_1 + R_2 - R_4 - R_5$
	ring	deformation	$S_{15} = R_1 - R_2 + R_3 - R_4 + R_5 - R_6$
	ring	deformation	$S_{16} = R_1 - R_2 + R_4 - R_5$
	ring	deformation	$S_{17} = R_1 - R_2 - 2R_3 - R_4 + R_5 + 2R_6$
	ring	deformation	$S_{18} = \alpha_1 - \alpha_2 + \alpha_3 - \alpha_4 + \alpha_5 - \alpha_6$
	ring	deformation	$S_{19} = 2\alpha_1 - \alpha_2 - \alpha_3 - 2\alpha_4 - \alpha_5 - \alpha_6$
	ring	deformation	$S_{20} = \alpha_2 - \alpha_3 + \alpha_5 - \alpha_6$
	P=X	stretch	$S_{21} = B$
	PCl$_2$	symmetric stretch	$S_{22} = s_1 + s_2$
	PCl$_2$	deformation (scissor)	$S_{23} = 4\delta - \varepsilon_1 - \varepsilon_2 - \pi_1 - \pi_2$
	PCl$_2$	rock	$S_{24} = \varepsilon_1 - \varepsilon_2 + \pi_1 - \pi_2$
	ring-P	bend (in-plane)	$S_{25} = \beta_1 - \beta_2$
	ring-PX	bend (in-plane)	$S_{26} = 5\theta - \varepsilon_1 - \varepsilon_2 - \pi_1 - \pi_2 - \delta$

Species		Description	Symmetry coordinate
A″	β-CH	deformation	$S_{27} = \lambda_1$
	β-CH	deformation	$S_{28} = \lambda_2$
	ring-P	deformation	$S_{27} = \eta_2$
	γ-CH	deformation	$S_{30} = \lambda_3$
	γ-CH and δ-CH	deformation	$S_{31} = \lambda_4 \cos \Phi + \eta_4 \sin \Phi$
	γ-CH and δ-CH	deformation	$S_{32} = -\lambda_4 \sin \Phi + \eta_4 \cos \Phi$
	ring	deformation	$S_{33} = \kappa_1 - \kappa_2 + \kappa_3 - \kappa_4 + \kappa_5 - \kappa_6$
	ring	deformation	$S_{34} = \kappa_1 - \kappa_3 + \kappa_4 - \kappa_6$
	ring	deformation	$S_{35} = \kappa_1 - 2\kappa_2 + \kappa_3 + \kappa_4 - 2\kappa_5 + \kappa_6$
	PCl_2	antisymmetric stretch	$S_{36} = s_1 - s_2$
	PCl_2	wag	$S_{37} = \varepsilon_1 + \varepsilon_2 - \pi_1 - \pi_2$
	PCl_2	twist	$S_{38} = \varepsilon_1 - \varepsilon_2 - \pi_1 + \pi_2$
		antisymmetric stretch	$S_{39} = \tau$

Our assignments agree in the major contributions to each line with those given in[31,32]; however, there are discrepancies in the minor ones, where we assume our assignments, which are based mainly on PED calculations, to be more accurate. The experimental papers use a force-field method and do not even yield the cis conformer as the most stable one, but a near-cis one.

As the tables show, with the exception of the lowest lines, the torsional mode, the errors of our calculated wavenumbers are all smaller than 9%, except the PCl_2 symmetric stretch in the gauche conformer of VS, which has an error of 16%. However, some lines assigned to the gauche conformers[31,32] belong to modes of a rather small intensity, making the assignments given in[31,32] at least doubtful in some cases. The errors in most of the lines range between 0 and 5% making the agreement rather good. The torsions – probably due to their non-linearity – show errors of 12 and 18%.

In the cis derivative of VO the PED of most of the lines shows at most two symmetry coordinates which are contributing more than 10% to the PEDs. Only five lines have three symmetry coordinates contributing, and two of them contain even four coordinates. Entirely pure vibrations are the

Table VIII

Symmetry species, s, theoretical wavenumbers, k (in cm^{-1}), experimental wavenumbers[31] (that at 992 cm^{-1} is from the gas phase, all others are from the liquid phase), k_e (in cm^{-1}), error percentage, e (in %), infrared intensities, I (in km mol^{-1}), Raman activities A (in Å^4 amu^{-1}), depolarization ratios, ρ, as calculated by the DFT/B3LYP method in 6-311G** basis set, and the potential energy distribution, PED, among the symmetry coordinates (only those larger than 10% are given), calculated with our program for cis and gauche dichloro-(vinyl)phosphine oxide

s	k	k_e	e	I	A	ρ	PED
				cis Dichloro(vinyl)phosphine oxide			
A″	88	100	12	0.1	7.3	0.75	89% S_{21}
A′	172	183	6	0.1	2.5	0.69	44% S_{11}, 26% S_{12}, 16% S_{13}, 13% S_{10}
A″	195	–	–	1.4	5.9	0.75	76% S_{17}
A′	209	215	3	1.9	4.3	0.74	54% S_{11}, 19% S_{13}, 13% S_{12}, 12% S_{10}
A′	307	315	0.3	24.4	4.4	0.55	66% S_{10}, 16% S_{13}, 10% S_5
A″	315	339	7	0.9	4.6	0.75	54% S_{16}, 28% S_{15}, 12% S_{17}
A′	375	396	5	6.0	17.9	0.11	60% S_4, 19% S_{12}, 15% S_{13}
A″	498	480	4	138.3	4.8	0.75	66% S_{15}, 13% S_{20}
A′	533	525	2	109.6	8.1	0.01	35% S_4, 34% S_{12}, 23% S_{13}
A″	625	613	2	173.0	6.3	0.75	53% S_{20}, 21% S_{16}, 18% S_{18}
A′	719	740	3	92.3	2.0	0.31	77% S_5
A″	1008	793	4	9.0	0.3	0.75	71% S_{18}, 26% S_{20}
A″	1028	895	4	43.3	0.4	0.75	97% S_{19}
A′	1039	992	4	0.8	3.9	0.75	62% S_9, 27% S_{14}
A′	1284	1254	2	57.8	5.7	0.75	37% S_6, 35% S_{14}, 16% S_9
A′	1293	1273	2	88.5	14.9	0.09	58% S_6, 31% S_{14}
A′	1429	1400	2	21.3	23.1	0.35	78% S_8, 16% S_7
A′	1657	1599	4	5.3	23.9	0.14	72% S_7, 21% S_8
A′	3140	3013	4	2.4	113.5	0.17	98% S_3
A′	3182	3042	5	0.4	85.0	0.31	96% S_1
A′	3232	3100	4	0.3	78.6	0.62	98% S_2

TABLE VIII
(Continued)

s	k	k_e	e	l	A	ρ	PED
				gauche Dichloro(vinyl)phosphine oxide			
A	70	–	–	0.1	7.8	0.74	100% S_{21}
A	174	–	–	0.9	5.5	0.72	43% S_{17}, 34% S_{11}, 13% S_{16}
A	180	–	–	0.1	3.3	0.74	43% S_{11}, 23% S_{17}, 11% S_{13}, 11% S_{12}
A	233	246	5	1.0	3.7	0.34	36% S_{10}, 23% S_{12}, 21% S_{11}
A	299	–	–	3.6	5.5	0.75	46% S_{16}, 25% S_{17}, 14% S_{15}
A	324	–	–	21.1	5.9	0.63	39% S_{12}, 37% S_{10}, 12% S_4
A	400	–	–	17.9	5.6	0.60	46% S_{13}, 29% S_{15}, 13% S_{10}
A	442	414	7	58.0	17.7	0.02	79% S_4
A	525	549	4	175.2	4.1	0.62	51% S_{15}, 18% S_{16}
A	619	–	–	115.6	6.4	0.48	58% S_{20}, 21% S_{18}
A	715	–	–	105.2	0.7	0.37	69% S_5
A	997	–	–	20.4	0.4	0.71	72% S_{18}, 28% S_{20}
A	1012	–	–	34.7	0.4	0.75	100% S_{19}
A	1032	–	–	7.2	4.0	0.61	66% S_9, 23% S_{14}
A	1276	1283	0.5	92.1	20.0	0.12	57% S_6, 30% S_{14}
A	1301	1393	7	74.5	4.2	0.69	39% S_6, 39% S_{14}, 12% S_9
A	1436	–	–	28.4	21.9	0.44	78% S_8, 15% S_7
A	1668	1607	4	3.4	24.3	0.15	72% S_7, 20% S_8
A	3145	3050	3	1.8	81.7	0.29	86% S_3, 13% S_1
A	3161	–	–	1.2	146.8	0.22	85% S_1, 13% S_3
A	3234	–	–	0.5	69.4	0.61	99% S_2

torsion, PCl_2 twist, C–P stretch, and three C–H stretches. The lines with most contributions are all between 400 and 1300 cm^{-1}. In that area also the lines with the largest IR intensities are located, while largest Raman activities are found above 3000 cm^{-1} for C–H stretches. This does not correspond directly to Raman intensities since they are inversely proportional to the wavenumber and directly to the fourth power of the difference between the exciting laser light and the actual wavenumber of the line.

Table IX

Symmetry species, s, theoretical wavenumbers, k (in cm^{-1}), experimental wavenumbers[32] (all from liquid IR spectra, except for those at 98 and 170 cm^{-1} that are from liquid Raman spectrum), k_e (in cm^{-1}), error percentage, e (in %), infrared intensities, I (in km mol^{-1}), Raman activities, A (in $Å^4$ amu^{-1}), depolarization ratios, ρ, as calculated by the DFT/B3LYP method in 6-311G** basis set, and the potential energy distribution, PED, among the symmetry coordinates (only those larger than 10% are given), calculated with the program for cis and gauche dichloro(vinyl)phosphine sulfide

s	k	k_e	e	I	A	ρ	PED
			cis Dichloro(vinyl)phosphine sulfide				
A″	80	98	18	0.1	7.2	0.75	89% S_{21}
A′	156	170	9	0.1	5.4	0.72	45% S_{12}, 41% S_{11}, 11% S_{13}
A″	172	181	5	0.2	11.5	0.75	88% S_{17}
A′	206	214	4	2.6	5.4	0.73	55% S_{11}, 19% S_{12}, 14% S_{13}
A″	237	254	7	0.1	4.3	0.75	78% S_{16}, 11% S_{15}
A′	245	–	–	11.4	7.0	0.63	82% S_{10}
A′	355	378	6	18.4	24.8	0.03	56% S_4, 28% S_{13}
A″	452	457	1	122.9	11.1	0.75	85% S_{15}
A′	466	502	7	47.6	14.3	0.04	36% S_{13}, 30% S_4, 19% S_{12}, 11% S_6
A″	614	584	5	92.0	5.4	0.75	64% S_{20}, 20% S_{18}, 11% S_{16}
A′	633	658	4	124.5	7.8	0.49	44% S_5, 41% S_6
A″	764	764	0	144.1	5.4	0.43	44% S_6, 38% S_5
A″	997	958	4	12.3	0.3	0.75	75% S_{19}, 24% S_{20}
A″	1017	982	4	39.3	0.1	0.75	100% S_{19}
A′	1031	1010	2	13.2	4.4	0.42	65% S_9, 23% S_{14}
A′	1287	1260	2	4.2	8.6	0.23	70% S_{14}, 21% S_9
A′	1425	1380	3	28.2	16.5	0.42	80% S_8, 16% S_7
A′	1659	1590	4	2.0	31.0	0.19	75% S_7, 20% S_8
A′	3139	3010	4	2.0	108.9	0.17	97% S_3
A′	3174	3034	5	1.0	110.4	0.29	95% S_1
A′	3230	3094	4	0.1	80.0	0.51	98% S_2

TABLE IX
(Continued)

s	k	k_e	e	l	A	ρ	PED
				gauche Dichloro(vinyl)phosphine sulfide			
A	68	–	–	0.2	7.9	0.75	100% S_{21}
A	160	–	–	0.5	8.5	0.75	52% S_{11}, 24% S_{12}, 19% S_{17}
A	167	–	–	0.5	6.0	0.73	72% S_{17}, 12% S_{11}
A	212	–	–	0.5	8.7	0.68	59% S_{16}, 14% S_{13}
A	227	–	–	0.6	4.4	0.56	32% S_{12}, 24% S_{11}, 16% S_{16}, 13% S_{10}
A	244	–	–	10.8	9.2	0.67	67% S_{10}, 16% S_{12}
A	376	394	5	19.2	16.4	0.20	40% S_{13}, 27% S_{15}
A	404	480	16	55.9	24.5	0.07	74% S_4
A	477	520	8	128.8	6.9	0.75	54% S_{15}, 15% S_{13}, 15% S_{16}
A	594	603	1	37.7	4.9	0.38	58% S_{20}, 17% S_{18}, 11% S_6
A	672	–	–	133.5	4.2	0.48	42% S_5, 21% S_6
A	747	778	4	176.1	17.5	0.41	56% S_6, 33% S_5
A	992	–	–	14.1	0.5	0.69	76% S_{18}, 24% S_{20}
A	1003	–	–	38.1	0.4	0.73	100% S_{19}
A	1030	–	–	5.6	3.8	0.55	69% S_9, 22% S_{14}
A	1290	–	–	2.5	9.3	0.17	71% S_{14}, 20% S_9
A	1432	–	–	21.8	32.9	0.42	80% S_8, 15% S_7
A	1661	1600	4	0.9	44.3	0.19	74% S_7, 19% S_8
A	3144	–	–	1.4	101.8	0.27	88% S_3, 10% S_1
A	3163	–	–	1.4	120.1	0.23	88% S_1, 11% S_3
A	3235	–	–	0.3	79.2	0.60	99% S_2

The situation is very similar in the gauche conformer, where the pure motions are the torsion, CH_2 symmetric stretch, PCl_2 symmetric stretch, CH_2 deformation I, and CH_2 antisymmetric stretch. Again, the largest IR intensities are found between 300 and 1500 cm^{-1}, while the largest Raman activities are above 3000 cm^{-1}. In the sulfide conformations the situation is

Table X

Symmetry species, s, DFT wavenumbers, k (in cm^{-1}), infrared intensities, I (in km mol^{-1}), Raman activities, A (in $Å^4$ amu^{-1}), depolarization ratios, ρ, as calculated by the DFT method in 6-311G** basis set, and the potential energy distribution, PED (only those larger than 10% are given), for planar dichloro(phenyl)phosphine oxide and sulfide

s	k	I	A	ρ	PED
				Dichloro(phenyl)phosphine oxide	
A″	35	0.0	7.0	0.75	100% S_{39}
A″	84	0.0	8.1	0.75	54% S_{29}, 26% S_{38}, 15% S_{37}
A′	127	0.4	1.7	0.65	39% S_{25}, 25% S_{24}, 23% S_{26}
A′	192	2.2	4.0	0.75	86% S_{23}, 12% S_{25}
A″	219	0.2	1.0	0.75	55% S_{38}, 30% S_{34}
A′	258	11.3	5.6	0.27	36% S_{24}, 2% S_6, 10% S_{19}
A″	311	1.1	5.6	0.75	47% S_{37}, 29% S_{36}, 12% S_{38}, 11% S_{34}
A′	334	0.4	8.5	0.29	41% S_{26}, 33% S_{22}, 18% S_{25}
A″	407	0.3	0.2	0.75	94% S_{35}
A′	407	12.8	10.1	0.00	29% S_{24}, 26% S_{22}, 17% S_6, 13% S_{19}
A″	458	19.6	2.5	0.75	34% S_{34}, 30% S_{36}, 24% S_{29}
A′	527	207.1	12.1	0.05	38% S_{22}, 24% S_{26}, 18% S_{19}
A″	543	263.5	5.0	0.75	41% S_{36}, 35% S_{37}, 17% S_{29}
A′	630	0.3	4.9	0.73	89% S_{20}
A″	703	39.4	0.0	0.75	71% S_{23}, 19% S_{29}
A′	725	41.0	4.3	0.39	47% S_{19}, 27% S_6
A″	758	28.6	0.5	0.75	73% S_{32}, 16% S_{28}
A″	863	0.1	0.3	0.75	52% S_{30}, 47% S_{27}
A″	952	0.4	0.1	0.75	64% S_{28}, 22% S_{32}, 13% S_{31}
A″	998	0.2	0.0	0.75	48% S_{27}, 41% S_{30}
A′	1015	1.9	33.8	0.10	56% S_{18}, 44% S_{12}
A″	1022	0.0	0.1	0.75	78% S_{31}, 12% S_{28}, 10% S_{23}
A′	1044	0.5	13.6	0.09	37% S_{14}, 23% S_{12}, 22% S_{18}
A′	1107	5.0	0.2	0.55	51% S_{17}, 19% S_8, 15% S_{11}

Table **X**
(Continued)

s	k	l	A	ρ	PED
A′	1116	52.0	11.8	0.16	25% S_{14}, 21% S_{12}, 18% S_6, 13% S_{18}, 10% S_7
A′	1186	0.2	4.2	0.75	40% S_{10}, 34% S_{11}, 14% S_{15}
A′	1210	2.9	3.5	0.68	38% S_9, 36% S_7, 26% S_{13}
A′	1286	149.5	18.2	0.12	94% S_{21}
A′	1326	0.8	0.2	0.49	69% S_{15}, 17% S_{10}
A′	1357	4.0	0.6	0.39	62% S_8, 15% S_{15}, 11% S_{11}
A′	1473	22.8	1.4	0.66	34% S_{17}, 28% S_{11}, 27% S_{10}
A′	1514	2.1	0.0	0.51	35% S_7, 33% S_{14}, 32% S_9
A′	1618	0.2	5.4	0.70	68% S_{16}, 11% S_{11}
A′	1630	4.6	33.3	0.61	68% S_{13}, 12% S_7, 10% S_9
A′	3173	0.8	44.9	0.68	53% S_5, 34% S_4, 11% S_2
A′	3182	2.8	80.6	0.75	43% S_1, 23% S_3, 20% S_2, 13% S_5
A′	3189	5.0	77.6	0.70	40% S_2, 36% S_3, 14% S_5
A′	3197	5.5	57.6	0.23	40% S_1, 37% S_3, 15% S_4
A′	3203	10.6	277.2	0.13	45% S_4, 29% S_2, 12% S_5, 11% S_1

Dichloro(phenyl)phosphine sulfide

s	k	l	A	ρ	PED
A″	28	0.0	4.8	0.75	100% S_{39}
A″	85	0.0	7.6	0.75	56% S_{29}, 23% S_{38}, 14% S_{37}
A′	120	0.2	3.2	0.74	42% S_{26}, 28% S_{25}, 14% S_{23}, 14% S_{24}
A″	181	0.0	4.8	0.75	72% S_{38}, 10% S_{37}
A′	189	2.1	4.1	0.74	78% S_{23}, 14% S_{25}
A′	206	6.6	6.7	0.67	47% S_{24}, 24% S_{26}, 17% S_6
A″	254	0.0	8.7	0.75	51% S_{37}, 28% S_{34}, 15% S_{36}
A′	303	2.8	8.2	0.20	34% S_{25}, 27% S_{22}, 21% S_{26}
A′	355	12.9	22.5	0.03	28% S_{22}, 21% S_6, 15% S_{24}, 14% S_{21}, 11% S_{19}
A″	407	0.3	0.3	0.75	94% S_{35}
A″	439	62.7	7.6	0.75	58% S_{36}, 21% S_{34}, 15% S_{29}

TABLE X
(Continued)

s	k	l	A	ρ	PED
A′	476	122.3	16.9	0.01	40% S_{22}, 19% S_{19}, 13% S_6, 12% S_{26}
A″	498	129.7	3.6	0.75	32% S_{29}, 25% S_{36}, 22% S_{37}, 16% S_{34}
A′	629	2.6	6.0	0.71	88% S_{20}
A′	686	103.6	11.3	0.29	40% S_{21}, 34% S_{19}
A″	698	29.5	0.0	0.75	74% S_{33}, 19% S_{29}
A′	742	120.3	6.4	0.45	43% S_{21}, 21% S_{19}, 20% S_6
A″	756	36.3	0.7	0.75	73% S_{32}, 18% S_{28}
A″	857	0.0	0.5	0.75	50% S_{27}, 50% S_{30}
A″	947	0.2	0.2	0.75	65% S_{28}, 23% S_{32}, 11% S_{31}
A″	994	0.0	0.2	0.75	46% S_{30}, 46% S_{27}
A′	1015	2.8	32.1	0.11	62% S_{18}, 38% S_{12}
A′	1020	0.0	0.1	0.75	84% S_{31}, 11% S_{28}
A′	1043	0.1	26.5	0.12	32% S_{14}, 32% S_{12}, 20% S_{18}
A′	1104	55.4	20.0	0.15	32% S_{14}, 21% S_{12}, 18% S_6, 11% S_{18}
A′	1110	1.0	0.4	0.73	53% S_{17}, 17% S_8, 15% S_{11}
A′	1186	0.2	5.1	0.75	41% S_{10}, 34% S_{11}, 13% S_{15}
A′	1213	5.2	4.4	0.72	38% S_9, 37% S_7, 25% S_{13}
A′	1324	1.4	0.2	0.46	69% S_{15}, 16% S_{10}
A′	1356	7.5	1.2	0.47	61% S_8, 16% S_{15}, 10% S_{11}
A′	1471	25.5	2.4	0.69	32% S_{17}, 29% S_{10}, 28% S_{11}
A′	1512	3.1	1.1	0.56	37% S_{24}, 31% S_{14}, 31% S_9
A′	1617	0.2	2.9	0.74	68% S_{16}, 11% S_{11}
A′	1626	3.2	54.3	0.54	69% S_{13}, 12% S_7, 11% S_9
A′	3174	0.8	50.1	0.73	55% S_5, 37% S_4
A′	3183	2.9	94.3	0.75	41% S_1, 41% S_3, 13% S_2
A′	3189	4.5	68.9	0.56	45% S_2, 25% S_3, 22% S_5
A′	3198	5.9	65.4	0.22	48% S_1, 33% S_3, 13% S_4
A′	3203	12.1	262.1	0.12	41% S_4, 35% S_2, 12% S_5

more or less the same as in the oxides, although the Raman activities in the lower wavenumber region in the sulfides tend to be somewhat larger than in the oxides, because of the contributions of the S atom, which lead to higher polarizabilities.

In the two phenyl derivatives the normal modes are in most cases composed of far more symmetry coordinates than in the vinyl derivatives. The largest IR intensities occur also here between 400 and 1500 cm^{-1} in the lower wavenumber regions where the skeletal vibrations show up. The largest Raman activities occur again in the region of C–H stretches. The torsions have much smaller wavenumbers in the phenyl derivatives than in the vinyl ones, probably because of a smaller interaction between PXCl$_2$ and the phenyl groups.

Replot of Experimental Vibrational Spectra

The calculation of theoretical vibrational spectra from the Gaussian data is described in Appendix 1S in the supplementary material. In order to obtain two comparable spectra from our experimental and the theoretical infrared and Raman spectra of PO (in the case of the vinyl derivatives we have the experimental spectra in form of tables from the literature), we have replotted the experimental spectra. We obtained the wavenumbers and peak intensities for each line from the experimental IR spectrum and, in order to replot it, we have assumed a constant line width $\Delta k = 10$ cm^{-1} in both spectra. For the experimental one we assumed a Lorentzian line shape for each of the lines, j,

$$L_j(k) = \frac{A_j}{\pi} \frac{\Delta k/2}{(k - k_j)^2 + (\Delta k/2)^2} \tag{3}$$

where the peak heights I_j can be measured from the experimental spectra and thus

$$I_j = L_j(k_j) = \frac{A_j}{\pi \Delta k/2} . \tag{4}$$

From this follows

$$A_j = \frac{1}{2} I_j \Delta k \pi \tag{5}$$

where I_j is the distance between the peak of the line and the base line of the experimental spectrum. The final spectrum is then the superposition of all experimental lines j

$$T(k) = -\sum_j \frac{I_j \, \Delta k/2}{(k - k_j)^2 + (\Delta k/2)^2} \tag{6}$$

and $T(k)$ is rescaled such that the largest absolute value of the transmittance is equal to unity. The Raman spectrum is treated in the same way, just with intensity instead of transmittance.

DISCUSSION OF SPECTRA

In Fig. 5 we show the calculated IR and Raman spectra of the mixture composed of 91.4% cis and 8.6% gauche conformer of dichloro(vinyl)phosphine oxide, based on Gibbs energies (298.15 K, 1 bar).
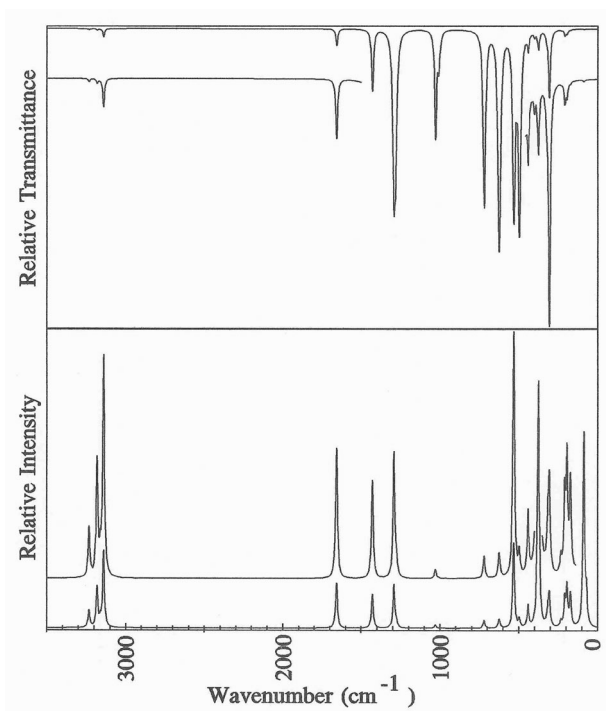

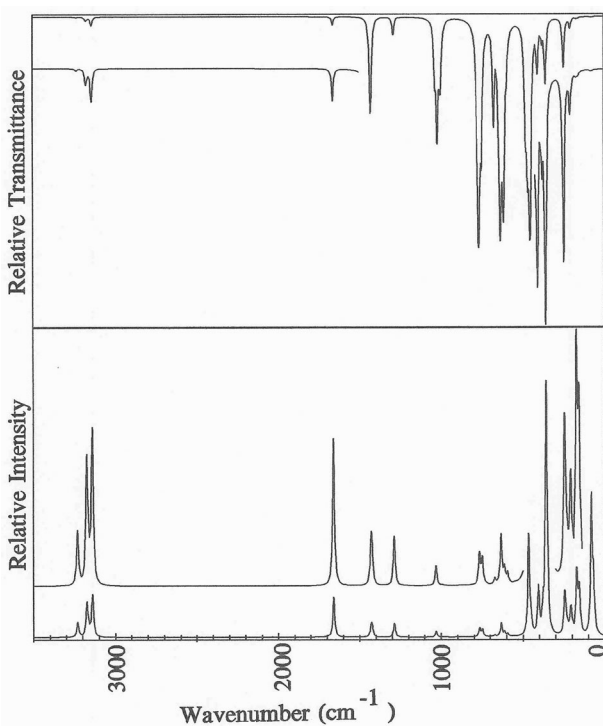
FIG. 5
IR (upper panel) and Raman (lower panel) spectra of a mixture (298.15 K, based on Gibbs energies) of 91.4% cis conformer with 8.6% gauche conformer of dichloro(vinyl)phosphine oxide, calculated by the DFT/B3LYP method in a 6-311G** basis set

As mentioned above, the bands in the skeletal or fingerprint region of the molecule show the largest IR intensities. In the Raman spectrum the torsion has clearly the second-largest intensity, while the largest intensity is found with a highly mixed band at 375 cm^{-1} which is built from 60% PCl$_2$ symmetric stretch, 19% CPO bend, and 15% CCP bend, having the largest polarizabilities. Another band of appreciable intensity is near 534 cm^{-1}, which has also a large IR intensity and consists of the same components as the former one with 35% PCl$_2$ symmetric stretch, 34% CPO bend, and 23% CCP bend.

Figure 6 shows the calculated IR and Raman spectra of the mixture composed of 80.8% cis and 19.2% gauche conformer of dichloro(vinyl)phosphine sulfide, based again on Gibbs energies (298.15 K, 1 bar).

FIG. 6
IR (upper panel) and Raman (lower panel) spectra of a mixture (298.15 K, based on Gibbs energies) of 80.8% cis conformer with 19.2% gauche conformer of dichloro(vinyl)phosphine sulfide, calculated by the DFT/B3LYP method in a 6-311G** basis set

The spectra have similar appearance as those of the oxide. Also the highest intensity lines in the spectra belong to the same mixture of symmetry coordinates. However, relative intensities in the oxide differ from those of the sulfide.

In the case of dichloro(phenyl)phosphine oxide we were able to find experimental IR and Raman spectra in the Internet[33]. As described above, we have replotted these spectra and in Fig. 7 we show the experimental together with the DFT IR spectrum.

Since here we have two identical planar conformers, the theoretical spectrum is not from a mixture. As expected, the P=O (S_{21}) stretch around 1300 cm^{-1} is one of the most characteristic bands due to the large charge separation in the bond, leading to a large dipole moment. In the theoretical
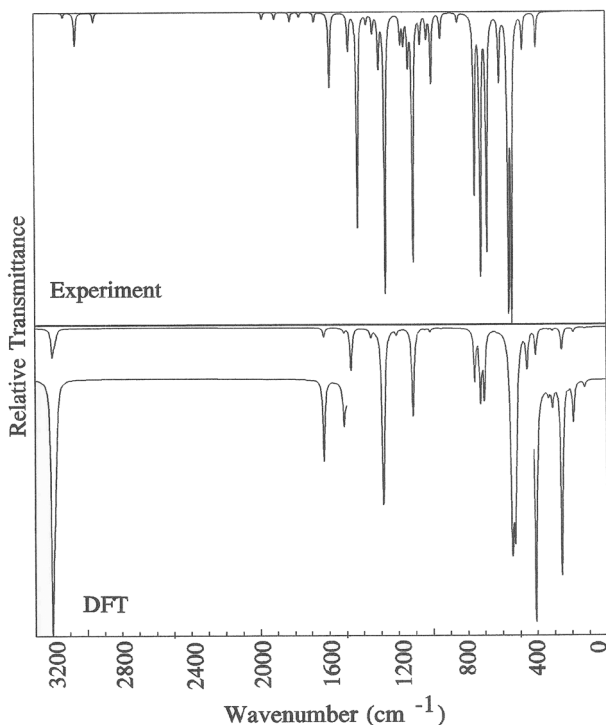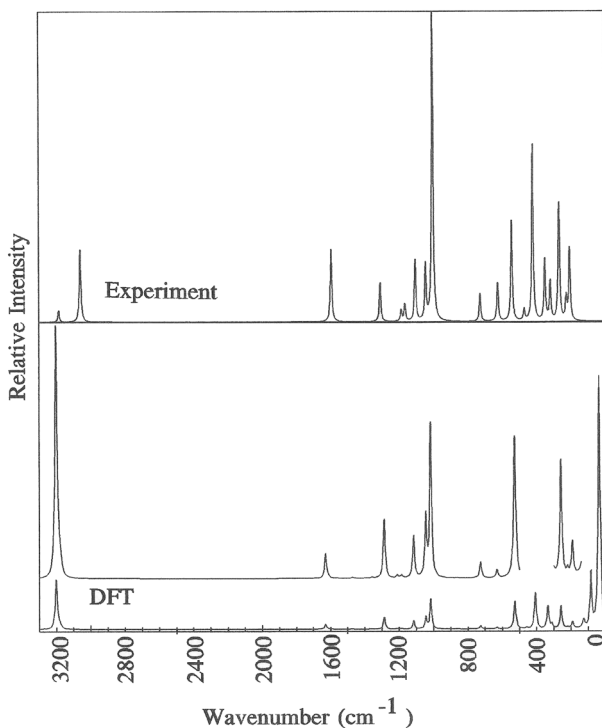

Fig. 7
IR spectrum of dichloro(phenyl)phosphine oxide as calculated by the DFT/B3LYP method in a 6-311G** basis set (lower panel) and the experimental spectrum (upper panel) which starts out at ca. 400 cm^{-1} and is replotted with a line width of 10 cm^{-1} in order to be better comparable with our theoretical spectrum

spectrum of PS, the P=S stretch appears at lower wavenumbers due to the weaker bond and with much smaller intensity because of the smaller charge separation. Between the wavenumbers 400 and 800 cm⁻¹ another very intense group of lines is found which contains PCl_2 vibrations, namely stretching and wagging. Obviously the DFT spectrum reproduces the experimental one remarkably well, showing the same overall pattern. Relative intensities are differing from each other, but that has to be expected. However, the high-intensity lines are all shown with comparable strength and in more or less similar locations. The agreement between experiment and theory is unexpectedly good.

In Fig. 8 we show, in the same way, experimental and DFT Raman spectra of the same molecule. The most characteristic line of largest intensity is

FIG. 8

Raman spectrum of dichloro(phenyl)phosphine oxide as calculated by the DFT/B3LYP method in a 6-311G** basis set (lower panel) and the experimental spectrum (upper panel) which starts out at ca. 200 cm⁻¹ and is replotted with a line width of 10 cm⁻¹ in order to be better comparable with our theoretical spectrum

found around 1000 cm^{-1}, both experimentally and theoretically. As expected, it is composed of ring breathing (S_{12}) and ring deformation (S_{18})

In this case the agreement is as good as in the former spectra. The seemingly different intensities are due to the fact that the lines of the highest intensity in the DFT spectrum (the lowest ones) are not included in the experimental one. However, as in the IR case, also the Raman spectra are in almost one-to-one correspondence.

The good agreement between experiment and DFT in the case of dichloro-(phenyl)phosphine oxide encourages us to show our predicted DFT spectra for the sulfide in Fig. 9.

The spectra again show some similarities to the corresponding spectra of the oxide as we observed in case of the vinyl compounds. We are quite convinced that the spectra in Fig. 9 are rather good predictions of IR and Raman spectra of dichloro(phenyl)phosphine sulfide.
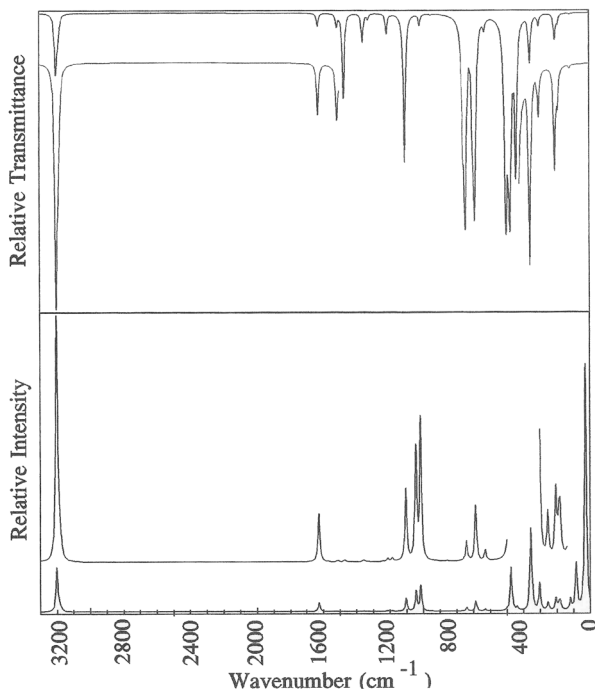

FIG. 9
IR (upper panel) and Raman (lower panel) spectra of the only stable planar conformer of dichloro(phenyl)phosphine sulfide, calculated by the DFT/B3LYP method in a 6-311G** basis set

CONCLUSION

Our main conclusion is that the structural properties of our dichloro(vinyl)-phosphine and dichloro(phenyl)phosphine oxides and sulfides are dominated not by conjugation but by electrostatic effects. Steric hindrance can also be excluded because such effects would stabilize the trans forms, which are actually transition states in the vinyl compounds and non-planar forms in the phenyl compounds, as it is in the case, e.g., of biphenyle. Vibrational spectra are reproduced rather well by DFT in both cases, which leads us to the conclusion that our prediction of the vibrational spectra of dichloro-(phenyl)phosphine sulfide should be at least a reasonable one.

Supporting Information Available

The calculated structural parameters, total energies, rotational constants and dipole moments of the molecules are available free of charge via doi:10.1135/cccc20080831.

REFERENCES

1. Keirns J., Curl, R. F., Jr.: *J. Chem. Phys.* **1968**, *48*, 3773.
2. Latypova R. G., Mamleev A. K., Gunderova L. N., Pozdeev N. M.: *Zh. Strukt. Khim.* **1976**, *17*, 849.
3. Durig J. R., Church J. S., Compton D. A. C.: *J. Chem. Phys.* **1979**, *71*, 1175.
4. Durig J. R., Brletic P. A., Church J. S.: *J. Chem. Phys.* **1982**, *76*, 1723.
5. Laskowski B. C., Jaffe R. L., Komornicki A.: *J. Chem. Phys.* **1985**, *82*, 5089.
6. Durig J. R.,Berry R. J., Groner P.: *J. Chem. Phys.* **1987**, *87*, 6303.
7. Durig J. R., Wang A. Y., Little T. S.: *J. Chem. Phys.* **1989**, *91*, 7361.
8. Durig J. R., Wang A. Y., Little T. S.: *J. Chem. Phys.* **1990**, *93*, 905.
9. Durig J. R., Brletic P. A., Li Y. S., Wang A. Y., Little T. S.: *J. Mol. Struct.* **1990**, *223*, 291.
10. Durig J. R., Groner C. V., Costner T. G., Wang A.: *J. Raman Spectrosc.* **1993**, *24*, 335.
11. De Mare G. R., Panchenko Y. N.: *J. Phys. Chem.* **1994**, *98*, 8315.
12. Durig J. R., Guirgis G. A., Jin Y.: *J. Mol. Struct.* **1996**, *380*, 31.
13. Badawi H. M.: *J. Mol. Struct. (THEOCHEM)* **1998**, *425*, 227.
14. Badawi H. M., Förner W.: *J. Mol. Struct. (THEOCHEM)* **2001**, *535* 103.
15. Backvall J., Chinchilla R., Najera C., Yus M.: *Chem. Rev.* **1998**, *98*, 2291.
16. Frisch M. J., Trucks G. W., Schlegel H. B., Scuseria G. E., Robb M. A., Cheeseman J. R., Zakrzewski V. G., Montgomery J. A., Jr., Stratmann R. E., Burant J. C., Dapprich S., Millam J. M., Daniels A. D., Kudin K. N., Strain M. C., Frakas O., Tomasi J., Barone V., Cossi M., Cammi R., Mennucci B., Pomelli C., Adamo C., Clifford S., Ochterski J.,

Petersson G. A., Ayala P. Y., Cui Q., Morokuma K., Malick D. K., Rabuck A. D., Raghavachari K., Foresman J. B., Cioslowski J., Ortiz J. V., Baboul A. G., Stefanov B. B., Liu G., Liashenko A., Piskorz P., Komaromi I., Gomperts R., Martin R. L., Fox D. T., Keith T., Al-Laham M. A., Peng C. Y., Nanayakkara A., Gonzalez C., Challacombe M., Gill P. M. W., Johnson B. G., Chen W., Wong W., Andres J. L., Head-Gordon M., Replogle E. S., Pople J. A.: *Gaussian 98*. Gaussian Inc., Pittsburgh (PA) 1998.

17. Wilson E. B., Decius J. C., Cross P. C.: *Molecular Vibrations*. McGraw-Hill, New York 1955.
18. Durig J. R., Berry R. J., Groner P.: *J. Chem. Phys*. **1987**, *87*, 6303.
19. Durig J. R., Daeyaert F. D., van der Veken B. J.: *J. Raman Spectrosc*. 1994, *25*, 869.
20. Durig J. R. , Guirgis G. A., Krutules K. A., Phan H., Stidham H. D.: *J. Raman Spectrosc.* **1994**, *25*, 221.
21. Chantry G. W. in: *The Raman Effect* (A. Anderson, Ed.), Vol. 1, Chap. 2. Marcel Dekker, New York 1971.
22. Durig J. R., Hizer T. J., Harlan R. J.: *J. Chem. Phys*. **1992**, *96*, 541.
23. Chatterjee K. K., Durig J. R.: *J. Mol. Struct*. **1995**, *351*, 25.
24. Durig J. R., Daeyaert F. D.: *J. Raman Spectrosc.* **1998**, *29*, 191.
25. Berning E. D., Katti V. K., Barnes L. C.: *J. Am. Chem. Soc.* **1999**, *121*, 1658.
26. Salama O., Raul G.-J., Jose M., de la Vega G.: *Int. J. Quantum Chem*. **2003**, *91*, 333.
27. Förner W., Badawi H. M.: *Collect. Czech. Chem. Commun.* **2007**, *72*, 15.
28. Förner W., Badawi H. M.: *Can. J. Anal. Sci. Spectrosc*. **2007**, *52*, 101.
29. Naumov V. A., Shagidullin S. A.: *Zh. Strukt. Khim*. **1976**, *17*, 304.
30. Hernandez-Laguna A., Sainz-Diaz C. I., Smeyers Y. G., de Paz J. L. G., Glavez-Ruano E.: *J. Phys. Chem*. **1994**, *98*, 1109.
31. Chernova A. V., Doroshkina G. M., Katsyuba S. A., Shagidullin R. R., Khailova N. A., Khairullin V. K.: *Izv. Akad. Nauk SSSR, Ser. Khim*. **1987**, *12*, 2729.
32. Chernova A. V., Doroshkina G. M., Katsyuba S. A., Shagidullin R. R., Khailova N. A., Khairullin V. K.: *Izv. Akad. Nauk SSSR, Ser. Khim*. **1988**, *3*, 568.
33. SDBSWeb: http://riodb01.ibase.aist.go.jp/sdbs/ (National Institute of Advanced Industrial Science and Technology, hit-no.: 2538); SDBS-No. 4178.